Driving Force Controller with Variable Slip Ratio Limiter for Electric Vehicle Considering Lateral Slip Based on Brush Model

Hiroyuki Fuse
The University of Tokyo
5-1-5, Kashiwanoha, Kashiwa, Chiba, 227-8561 Japan
Phone: +81-4-7136-3848
Fax: +81-4-7136-3848
Email: fuse.hiroyuki17@ae.k.u-tokyo.ac.jp

Hiroshi Fujimoto
The University of Tokyo
5-1-5, Kashiwanoha, Kashiwa, Chiba, 227-8561 Japan
Phone: +81-4-7136-4131
Fax: +81-4-7136-4132
Email: fujimoto@k.u-tokyo.ac.jp

***Abstract*—As one of EV's motion control methods, a driving force controller (DFC) with slip ratio limiter has been proposed in order to maintain the traction of tire effectively. The conventional controller has a slip ratio limiter for safety reason, but it did not consider lateral slip of tire during cornering. To deal with this problem, this paper proposes a DFC with variable slip ratio limiter based on brush model. The experimental results show that the proposed controller can work on both acceleration and deceleration cornering, with increase of lateral force and lateral acceleration, contributing to smoother cornering.**

***Keywords*—Electric Vehicle, vehicle dynamics, maneuverability, driving force controller, brush model, slip ratio control, grip margin**

I. Introduction

Nowadays, electric vehicle (EV) has gained great attention for its environmental friendliness. However, EV has problems in the driving range and charging time due to the limitation of energy storage. To deal with this problem, a lot of research has been investigated in order to extend the short range [1] [2].

While EV has a great potential for environmental problem, it can be also safer since it has several advantages in controllability and maneuverability [3]. They are

1) Fast torque control response within several milliseconds
2) Torque and driving force can be easily estimated
3) Capability of driving and regenerating
4) Capability of independent-four-wheel-drive (4WD) system

Using these advantages, a lot of traction control and motion stabilization methods have been proposed [4].

The authors' group has been proposed a driving force controller (DFC) [4]. The DFC directly controls slip ratio so that desired driving force can be obtained regardless of road condition. There is a slip ratio limiter that maintains the traction of tire for safer drive.

However, the previous DFC was only effective on straightways since the slip ratio limiter adopted constant value (Constant Slip Ratio Limiter; CSRL). There was a situation where enough amount of lateral force cannot be generated during the cornering when longitudinal slip is too large.

To improve the conventional DFC, the author proposed a driving force controller considering sideslip angle based on "λ–Method" tire model [5]. In the proposed method, the value of slip ratio limiter changes according to slip angle so that tire always keeps its traction even when cornering (Variable Slip Ratio Limiter; VSRL). However, the proposed method only deals with tire which has equal stiffness on longitudinal and lateral direction.

To deal with this problem, a DFC considering sideslip angle based on brush model was proposed [6]. It enables us to deal with wider range of tires which have different stiffness on longitudinal and lateral direction. Furthermore, this method also suggested that tire workload can be limited to a desired value so that tire lifetime can be extended. However, in [6], experimental verification was only conducted on acceleration with the reference tire workload limiter of 0.7, requiring more data for validity and effectiveness.

This paper reports further experimental results on both acceleration and deceleration modes. In addition, the simplified derivation of the VSRL of the DFC is proposed, while the former study obtained the equations of slip ratio limiter based on two equations since it adopted different definition of the slip ratio for both acceleration and deceleration. The structure of this paper is as follows. In the next section, tire model used in this paper is introduced. Next, the structure of the DFC is explained. Then, the VSRL of the DFC based on brush model with simplified derivation is proposed. Finally, experimental verification of the proposed method and its effectiveness are described.

II. Vehicle Model

A. Vehicle model

In this paper, we consider a vehicle that is capable of independent-4WD. Fig. 1 shows an illustration of the vehicle model. In the figure, a_x, a_y, V, β, γ, α, F_x, F_y, and δ_f are longitudinal, lateral acceleration, vehicle velocity, vehicle's

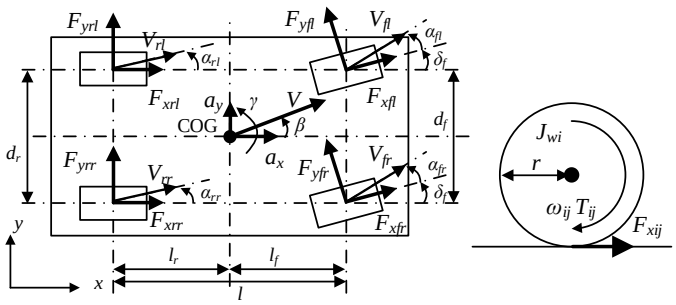

Fig. 1. Vehicle model.

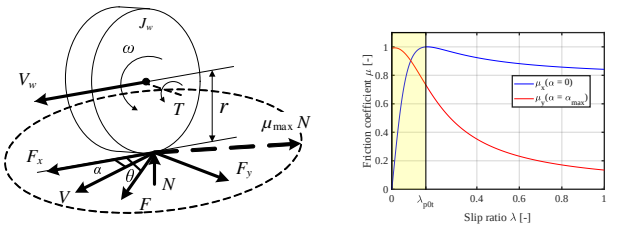

(a) Tire model. (b) λ–μ curve ($\alpha = 0$).

Fig. 2. Tire force model.

sideslip angle, yaw rate, sideslip angle, longitudinal force, lateral of each wheel, and front steering angle, respectively. The subscription of i will be f or r, indicating front or rear wheel, and j will be l or r, indicating left or right respectively.

B. Tire model

To get a better understanding of the DFC and the proposed method later, this section describes basic properties of tire forces and a brush model. Fig. 2(a) shows an illustration of the tire model. In the figure, α, F_x, F_y, J_ω, ω, T, and r are longitudinal and lateral forces, wheel's inertia, angular velocity, torque input, and radius of tire, respectively. Equation of rotation of wheel is given by

$$J_{\omega_i}\dot{\omega} = T - rF_x. \tag{1}$$

C. Friction Circle and Tire Workload

Assuming maximum friction coefficient $\mu_{\max}$, resultant force F, longitudinal force F_x, lateral force F_y, normal reaction force N, and the direction of resultant force θ, the following equations have to be satisfied.

$$F = \sqrt{F_x^2 + F_y^2} \le \mu_{\max} N \tag{2}$$

$$\theta = \tan^{-1}(F_y/F_x) \tag{3}$$

This concept is called a friction circle shown in Fig. 2(a) (dashed circle), indicating tire force has its limit determined by the condition of road and tire, and normal reaction force N acting on tire. Tire workload η is defined by

$$\eta = \sqrt{F_x^2 + F_y^2}/(\mu_{\max} N) \le 1. \tag{4}$$

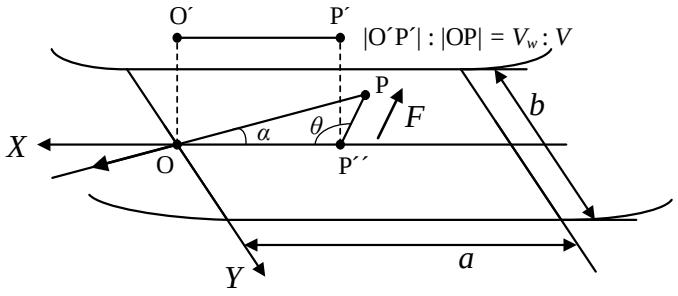

Fig. 3. Tread rubber distortion during deceleration cornering.

1) Generation of Tire Force: In general, longitudinal and lateral force are generated by slip ratio λ and sideslip angle α, respectively. In this paper, slip ratio λ is defined by

$$\lambda = (V_\omega - V)/\max(V_\omega, V), \tag{5}$$

where $V_\omega = r\omega$ and V is vehicle velocity. The relation between slip ratio λ and friction coefficient of road μ is nonlinear as shown in Fig. 2(b). The friction coefficient takes its maximum value $\mu_{\max}$ at a certain slip ratio called optimal slip ratio λ_{p0} when $\alpha = 0$.

D. Brush Model

Brush model assumes countless number of brush-shaped elastic body continuously on the surface of tire. Tire force and its moment are calculated based on the elastic deformation of the brush. Fig. 3 illustrates the deformation of tread rubber when braking with sideslip. a, b, C_x, C_y denote the length and width of contact area, longitudinal and lateral stiffness of the brush, respectively. By assuming that the longitudinal and lateral pressure distributions of contact area are quadratic and constant respectively, resultant force $F$is obtained as follows [7].

$$F(\lambda,\alpha) = \begin{cases} \mu_{\max} N s(3 - 3s + s^2), & [0 \le s \le 1] \\ \mu_{\max} N, & [s > 1] \end{cases} \tag{6}$$

where s is the normalized length of slipping area divided by a. When $s = 0$, tire is completely adhesive. When $s = 1$, all the contact area becomes slipping area. During deceleration, s and θ are given by

$$\theta(\lambda,\alpha) = -\tan^{-1}\left(\frac{\phi \tan\alpha}{\lambda}\right) \tag{7}$$

$$s(\lambda,\alpha) := K\frac{\sqrt{\lambda^2 + \phi^2\tan^2\alpha}}{1+\lambda} \tag{8}$$

$$K := a^2 b C_x/(6\mu_{\max} N), \quad C_y = \phi C_x \tag{9}$$

where K is a parameter determining s and ϕ is a stiffness ratio of longitudinal and lateral direction.

III. Driving Force Controller

A. Block Diagram and Structure

The block diagram of the DFC is shown in Fig. 4. The outer loop is a driving force loop and the inner loop is a slip ratio/wheel velocity loop that controls the slip ratio. From (1),

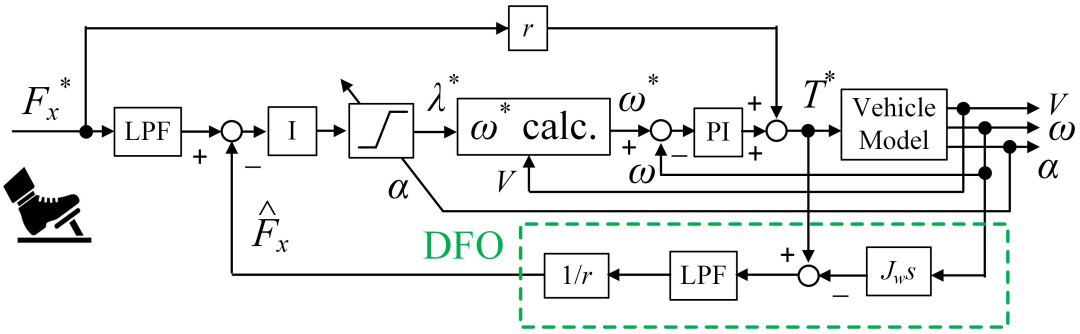

Fig. 4. Driving Force Controller with proposed variable slip ratio limiter.

the driving force of each wheel is estimated by a driving force observer (DFO). F_x^* is the reference longitudinal force and $\hat{F}_x$ is the estimated driving force. The definition of slip ratio has two cases on both acceleration and deceleration. For smoother control, new control input y is defined as

$$y = (V_\omega - V)/V. \tag{10}$$

This is the same definition as that of slip ratio for deceleration. The relationship between y and λ for acceleration is calculated as

$$y = \lambda/(1-\lambda). \tag{11}$$

y approximately equals to λ when $|\lambda| << 1$ and they are always one to one correspondence. From (10), the wheel velocity reference ${V_\omega}^*$ of the inner loop is calculated as

$$\begin{cases} {V_\omega}^* = (1+y)V & (V \geq \sigma) \\ {V_\omega}^* = V + y\sigma & (V < \sigma), \end{cases} \tag{12}$$

where σ is a small constant to prevent a problem of ${V_\omega}^* = 0$ when the vehicle stops $(V = 0)$.

As F_x^* is inputed, feedforward loop outputs approximately adequate torque reference which ignores the derivative of the angular speed. This secures fast response of the DFC. Inner slip ratio/wheel speed control loop adjusts slight error for precise output. As long as vehicle is on high traction road or F_x^* is not as large as the limit of tire force, DFC operates as a direct torque controller.

B. Slip Ratio Limiter and Traction Control

The equation of tire model (6) suggests that resultant force F is maximized when $s \geq 1$. However, for the controllability of vehicle maneuver and considering the general fact that F rather decreases if tire slips too much [8], $s \leq 1$ is desired. To achieve this, slip ratio's upper and lower limit $y_{\max}$ and $y_{\min}$ for the integrator of the DFC are added. With this saturation, traction can be retained by keeping the slip ratio within the range where μ is monotonic function of λ (see Fig. 2(b)) if we know certain value of the optimal slip ratio λ_{p0}, which is easy to estimate using an EV with IWM [9].

IV. Simplified Derivation of Variable Slip Ratio Limiter

This section derives VSRL that can limit tire workload η within desired value. The previous study [6] derived the upper and lower limiter of the slip ratio $y(\alpha)$ for both acceleration and deceleration modes from respectively defined equations of θ and K (this paper only shows that of deceleration). On the other hand, this paper only uses deceleration mode so that conversion to the slip ratio reference y will be unnecessary and omitted (It should be noted that the actual value of obtained VSRL for acceleration will be converted using (11)).

A. Derivation of Critical Condition ($s = \eta = 1$)

In this paper, "critical condition" indicates a set of slip ratio λ and sideslip angle α which satisfy $s = 1$ and $\eta = 1$, when tire force is effectively maximized. This section derives the critical condition used for the VSRL of the DFC.

1) Derivation of Parameters K and ϕ: K and ϕ are important parameters to be obtained. With the priori knowledge of an optimal slip ratio in case of acceleration λ_{p0t} [9], K is derived as following equation by substituting these conditions to (5) and (8).

$$K = 1/\lambda_{\mathrm{p0t}} \tag{13}$$

Stiffness ratio ϕ can be estimated by (3) and (7), with the measurement of F_x, F_y, λ, and α as follows.

$$\phi = -\frac{F_y \lambda}{F_x \tan\alpha} \tag{14}$$

2) Derivation of Critical Condition: Combined with (6), (8), and (13), we have the critical condition where $\eta = 1$ and $s = 1$ satisfy as follows.

$$\lambda_{\mathrm{p0t}} = \frac{\sqrt{\lambda^2 + \phi^2 \tan^2\alpha}}{(1+\lambda)} \tag{15}$$

By squaring both sides, it is easy to see that this is an implicit curve. If we solve (15) for λ, we have two solutions for the VSRL. Since $y = \lambda$ for deceleration, we obtain the upper and

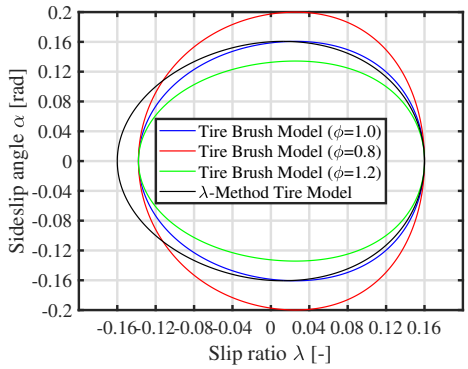

Fig. 5. Comparison of Critical Condition with different value of ϕ.

lower limit $y_{\max}$ and $y_{\min}$ of the VSRL as follows.

$$y_{\max}(\alpha) = \frac{\lambda_{\mathrm{p0t}}^2 + X_1}{1-\lambda_{\mathrm{p0t}}^2} \quad (|\alpha| \le \alpha_{\max}) \tag{16}$$

$$y_{\min}(\alpha) = \frac{\lambda_{\mathrm{p0t}}^2 - X_1}{1-\lambda_{\mathrm{p0t}}^2} \quad (|\alpha| \le \alpha_{\max}) \tag{17}$$

$$\tag{18}$$

$$X_1 := \sqrt{\lambda_{\mathrm{p0t}}^2 + (\lambda_{\mathrm{p0t}}^2 - 1)\phi^2 \tan^2\alpha} \tag{19}$$

$$\alpha_{\max} := \tan^{-1}\frac{\lambda_{\mathrm{p0t}}}{\phi\sqrt{1-\lambda_{\mathrm{p0t}}^2}} \tag{20}$$

Fig. 5 shows the implicit curves of the critical condition of λ and α with tire parameters of $\lambda_{\mathrm{p0t}} = 0.16$, $\phi = 0.8, 1, 1.2$. Three values of the stiffness ratio ϕ were tested to see the difference effectively.

For comparison, λ–α characteristic of the critical condition obtained by λ–Method [10] [5] is also shown in Fig. 5 ($\lambda_{\mathrm{p0t}} = 0.16$).

B. VSRL with Grip Margin ($s < 1$)

The last section derived the critical condition for the VSRL of DFC. The proposed VSRL can maintain and maximize tire's traction even during cornering. However, unless emergency situation when vehicle needs to maneuver in drastic manner fully using tire's limit, tire's slip should be as low as possible in order to reduce slip power dissipation and extend lifetime of tire. This section suggests a VSRL with certain grip margin of tire for this purpose.

Tire workload η is represented by s from (4) and (6) as follows.

$$\eta = s(3 - 3s + s^2), \quad [0 \le s \le 1] \tag{21}$$

This equation can be solved for s and given by

$$s = 1 - (1-\eta)^{\frac{1}{3}}, \quad [0 \le \eta \le 1] \tag{22}$$

If we give desired grip margin $m = 1 - \eta$, $s_{\lim}$ is derived by

$$s_{\lim} = 1 - m^{\frac{1}{3}}, \quad [0 \le m \le 1] \tag{23}$$

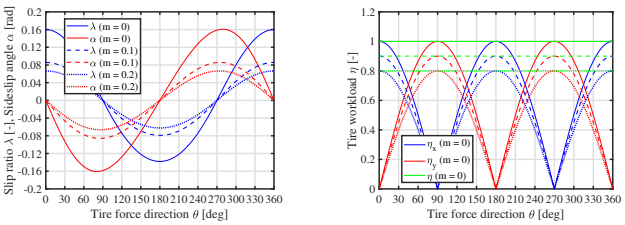

(a) $\lambda(\theta)$, $\alpha(\theta)$ curves. (b) $\eta(\theta)$ curves.

Fig. 6. Slip ratio, sideslip angle, and tire workload with grip margin $m = 0, 0.1, 0.2$.

TABLE I
EXPERIMENTAL CONDITION.

λ_{p0t}	ϕ	$\mu_{\max}$	m	V_{ref}
0.16	1.12	0.27	0	6 m/s

By liming $s \le s_{\lim}$, we can get desired grip margin m. To obtain slip ratio λ and sideslip angle α that satisfy given $s_{\lim}$, $s = s_{\lim}$ should be substituted instead of $s = 1$ to (15). In other words, all the term λ_{p0t} in the equations of the critical condition should be replaced by $s_{\lim}\lambda_{\mathrm{p0t}}$ instead as shown below.

$$y_{\max}(\alpha, s_{\lim}) = \frac{\phi^2\tan^2\alpha + X_2}{1 - X_2} \tag{24}$$

$$y_{\min}(\alpha, s_{\lim}) = \frac{s_{\lim}^2\lambda_{\mathrm{p0t}}^2 - X_2}{1 - s_{\lim}^2\lambda_{\mathrm{p0t}}^2} \tag{25}$$

$$X_2 := \sqrt{s_{\lim}^2\lambda_{\mathrm{p0t}}^2 + (s_{\lim}^2\lambda_{\mathrm{p0t}}^2 - 1)\phi^2\tan^2\alpha} \tag{26}$$

Fig. 6 shows λ, α, and η with desired grip margin $m = 0, 0.1, 0.2$. By reducing magnitude of λ and α compared to the critical condition, calculated η becomes smaller and the desired grip margin is attained.

V. EXPERIMENTAL VERIFICATION OF VSRL BASED ON BRUSH MODEL

We conducted an experiment using a real EV on acceleration and deceleration mode on slippery road shown in Fig. 7. The slippery road was emulated by polymer sheets with sprayed water on the surface. To focus on the effect of the VSRL, we used a slip ratio controller with the proposed VSRL shown in Fig. 8. The controller drives front wheels with the slip ratio reference value λ_{p0t}. As driver manually steers wheel and generates tire sideslip angle, the proposed VSRL limits the slip ratio reference to be $\lambda_{\mathrm{drv}}(\alpha)$. Desired tire grip margin m is set to be 0. Rear wheels are driven by a vehicle speed controller that maintains constant speed of V_{ref} = 6 m/s. Tab. I shows experimental condition. λ_{p0t}, ϕ, and $\mu_{\max}$ are obtained in advance [9] [11]. For comparison, acceleration cornering with constant slip ratio limiter was also carried out.

Fig. 7. Exp. setup.

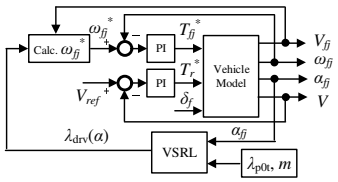

Fig. 8. VSRL controller.

TABLE II
VEHICLE SPECIFICATION.

Vehicle mass (including driver) M	910 kg
Wheelbase l	1.7 m
Distance from center gravity to front and rear axle l_f,l_r	l_f:1.0 m l_r:0.7 m
Gravity height $h_{\rm g}$	0.51 m
Front and rear wheel inertia J_{ω_f}, J_{ω_r}	1.24, 1.26 kg·m^2
Wheel radius r	0.302 m

A. Experimental Vehicle

In this study, we use an EV "FPEV2–Kanon" shown in Fig. 7 for experimental verification. The EV is equipped with a direct-drive in-wheel motor (IWM) in each wheel and capable of independent 4WD control. The equipped IWM has maximum power of 20 kW and speed of 1200 rpm. Tab. II shows the specification of the experimental vehicle.

B. Measurement and Estimation

We use an optical velocity sensor, acceleration sensor, yaw rate sensor, and wheel speed sensor for obtaining required information of vehicle maneuver. We used an AUTOBOX DS1103 for computation. The sampling rate for the experiment is 20 kHz. Lateral force F_y, sideslip angle α, and tire workload η were estimated by measured values by the sensors [10].

C. Results

Fig. 9 and Fig. 10 show experimental results of the acceleration mode with the CSRL and with a VSRL based on the brush model. These results only show those of the front left wheel. In case of the CSRL, slip ratio λ_{fl} is maintained around $\lambda_{\rm p0t} = 0.16$ regardless of the gradual increase of sideslip angle α_{fl} (Fig. 9(a)). On the other hand, in case of the VSRL, slip ratio λ_{fl} decreases (Fig. 10(a)). Because of this difference, the CSRL has larger longitudinal force F_{xfl} and smaller lateral force F_{yfl} compared to the VSRL when sideslip angle α_{fl} is large (Fig. 9(b) and Fig. 10(b)). It is clear on the difference of the lateral part of tire workload η_{yfl} (Fig. 9(c) and Fig. 10(c)). While η_{yfl} of the CSRL only reaches to 0.6, that of the VSRL to 0.7. In addition, lateral acceleration a_y has larger value on the VSRL (Fig. 9(d) and Fig. 10(d)). Therefore, the VSRL effectively increases lateral force and acceleration. Thanks to that, a smoother cornering and the enhancement of cornering ability can be achieved.

Fig. 11 shows experimental results of the deceleration mode with the VSRL. Like the results of the acceleration mode with the VSRL, slip ratio λ_{fl} changes according to sideslip angle α_{fl} (Fig. 11(a)). Lateral force F_{yfl} increases up to 400

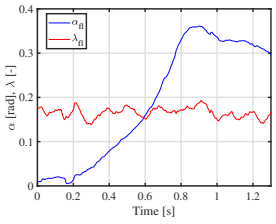

(a) Sideslip angle α_{fl} and slip ratio λ_{fl}.

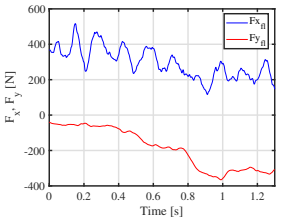

(b) Tire forces F_{xfl}, F_{yfl}.

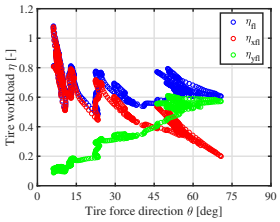

(c) Tire workload η_{fl}.

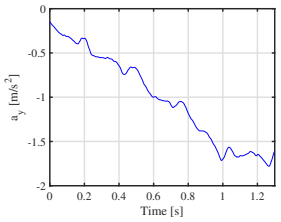

(d) Lateral acceleration a_y.

Fig. 9. Experimental results of acceleration cornering with constant slip ratio limiter (Conventional Method).

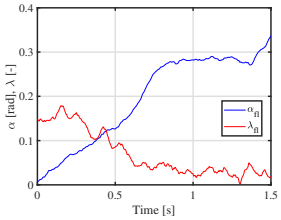

(a) Sideslip angle α_{fl} and slip ratio λ_{fl}.

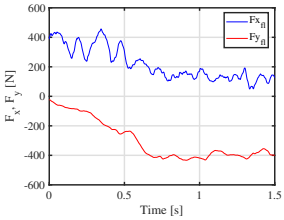

(b) Tire forces F_{xfl}, F_{yfl}.

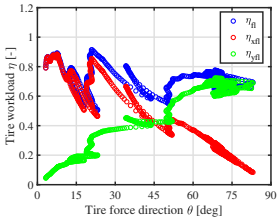

(c) Tire workload η_{fl}.

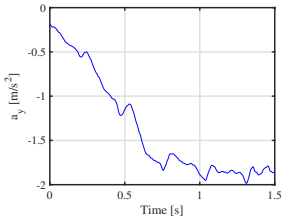

(d) Lateral acceleration a_y.

Fig. 10. Experimental results of acceleration cornering with variable slip ratio limiter (Proposed Method).

N with the decrease of longitudinal force F_{xfl} (Fig. 11(b)). Tire workload η_{yfl} also reaches up to 0.8 (Fig. 11(c)). This indicates that the VSRL also works on deceleration mode as much as acceleration mode.

One thing should be mentioned that tire workload does not reach 1.0 in any cases. An expected reason is that the given information $\mu_{\rm max} = 0.27$ was actually different during the experiments.

VI. Conclusion

This paper proposed a variable slip ratio limiter (VSRL) for a driving force controller based on brush model, especially for electric vehicle with four wheel independent drive system. With the proposed method, slip ratio is suppressed while

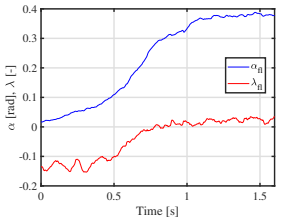

(a) Sideslip angle α_{fl} and slip ratio λ_{fl}.

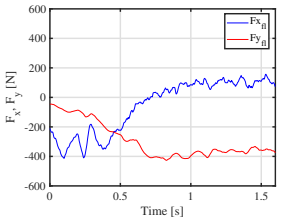

(b) Tire forces F_{xfl}, F_{yfl}.

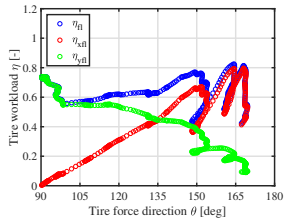

(c) Tire workload η_{fl}.

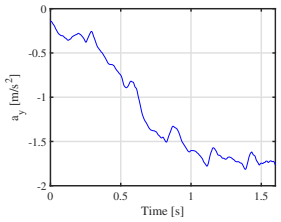

(d) Lateral acceleration a_y.

Fig. 11. Experimental results of deceleration cornering with variable slip ratio limiter (Proposed Method).

cornering so that greater lateral force can be generated for stable and smoother cornering, compared to the conventional constant slip ratio limiter. Experimental verifications on both acceleration and deceleration modes suggested the proposed VSRL can handle on the both modes, with the increase of lateral force and lateral acceleration.

VII. Acknowledgments

This research was partly supported by Industrial Technology Research Grant Program from New Energy and Industrial Technology Development Organization (NEDO) of Japan (number 05A48701d), the Ministry of Education, Culture, Sports, Science and Technology grant (number 22246057 and 26249061).

References

[1] Y. Ikezawa, et. al., "Range Extension Autonomous Driving for Electric Vehicles Based on Optimal Velocity Trajectory Generation and Front-Rear Driving-Braking Force Distribution," IEEJ J. Industry Applications, vol. 5, no. 3, pp. 228–235, 2016.

[2] G. Lovison, et. al.,"Secondary-side-only Control for High Efficiency and Desired Power with Two Converters in Wireless Power Transfer Systems,"IEEJ J. Industry Applications, vol. 6, no. 6, pp. 473–481, 2017.

[3] Y. Hori, "Future vehicle driven by electricity and control research on four-wheel-motored "UOT electric march II"", IEEE Trans. Industrial Electronics, 51, 5, pp. 954-962 (2004).

[4] M. Yoshimura and H. Fujimoto, "Driving torque control method for electric vehicle with in-wheel motors", IEEJ Transactions on Industry Applications, Vol. 131, No. 5, pp.1-8 (2010) (in Japanese).

[5] H. Fuse, H. Fujimoto. "Fundamental Study on Driving Force Control Method for Independent-Four-Wheel-Drive Electric Vehicle Considering Tire Slip Angle", IEEE conference IECON2018, 2018.

[6] H. Fuse, H. Fujimoto: "Driving Force Controller for Electric Vehicle Considering Sideslip Angle Based on Brush Model", IEEE 2019 International Conference on Mechatronics, Ilmenau, Germany (2019).

[7] O. Nishihara, et-al, "Estimation of Road Friction Coefficient Based on the Brush Model", Transactions of the Japan Society of Mechanical Engineers Series C 75(753), 1516-1524, 2009. (in Japanese).

[8] H. B. Pacejka and E. Bakker, "The Magic Formula Tyre Model," Vehicle System Dynamics: International Journal of Vehicle Mechanics and Mobility, Vol. 21, No. 1, pp. 1-18 (1992).

[9] H. Fuse, et.al. "Minimum-time Maneuver and Friction Coefficient Estimation Using Slip Ratio Control for Autonomously-Driven Electric Vehicle", IEEJ SAMCON2018, 2018.

[10] H. Fuse, H. Fujimoto, "Effective Tire Force Vector Control and Maximization Method for Independent-Four-Wheel-Drive Electric Vehicle, The 2018 IEEE International Transportation Electrification Conference & EXPO Asia-Pacific", Bangkok, Thailand, Session 8A2-2, Proceedings pp.54 (2018).

[11] K. Maeda, H. Fujimoto, Y. Hori, "Driving Force Control of Electric Vehicle Based on Optimal Slip Ratio Estimation Using brush model", JIASC, Vol. IV, pp. 137-140, 2012.

[12] K. Fujii, H. Fujimoto, "Traction Control based on Slip Ratio Estimation Without Detecting Vehicle Speed for Electric Vehicle", IEEE, Power Conversion Conference, 2007.